SPECTRAL CHARACTERISTICS OF RADIO NOISE AT LOW AND MEDIUM FREQUENCIES IN THE ANTARCTIC TOPSIDE IONOSPHERE

Kazuhiro AIKYO, Tadanori ONDOH, Ryo NISHIZAKI, Takashi MARUYAMA, Seiji IGI, Mikitoshi NAGAYAMA, Hisashi YABUUMA, Toshiyuki IDE

Radio Research Laboratories, 2–1, Nukui-Kitamachi 4-chome, Koganei-shi, Tokyo 184

and

Takeo HIRASAWA

National Institute of Polar Research, 9–10, Kaga 1-chome Itabashi-ku, Tokyo 173

***Abstract*:** The ISIS topside sounder data obtained at Syowa Sation, Antarctica, for the period from April 1976 to November 1977 are examined with emphasis on the noise spectra appearing on the Automatic Gain Control (AGC) data and on the ionograms.

The noise events were observed on 16 out of 88 ISIS-1 passes and on 8 out of 138 ISIS-2 passes. At high altitudes near ISIS-1 apogee, almost all of the noise events are due to auroral kilometric radiations (AKR). A special event of AKR observed in the dayside ionosphere is investigated in detail. The result shows that this cusp-associated AKR occurred in a large scale region of electron density depletion where the ratio of electron plasma frequency, f_N to electron gyrofrequency, f_H ranges from 0.1 to 0.05. At altitudes below 2900 km, two types of noise were observed; the whistler mode noise and the noise band appearing between the local f_N and f_T (upper hybrid resonance frequency). These noises are examined in connection with the local characteristic frequencies. The dependence of these noise intensities on the relationship between f_N and f_H is found to be in a qualitative agreement to Maggs' power flux calculation of the electrostatic noise using the plausible auroral electron beam models.

1. Introduction

In addition to the various aeronomical observations at Syowa Station, Antarctica, the telemetry reception of ISIS and NOAA signals has continued since April 1976 as a part of the Japanese IMS program, and a great amount of data has been accumulated in order to study the geophysical phenomena above the antarctic region. The preliminary analysis of ISIS-2 ionograms recorded at Syowa in 1976 has already revealed the seasonal variation of the electron density distributions (MATUURA *et al.*, 1977). For the period from April 1976 to January 1981 (the 17th–21st wintering parties of the Japanese Antarctic Research Expedition, JARE-17–JARE-21), the ISIS observations were made at Syowa on 1580 passes as shown in Table 1, in which the mixed mode

Table 1. Number of ISIS passes observed at Syowa Station.

Period	ISIS-1		ISIS-2	
	SDR	VLF	SDR	VLF
Apr. 1976–Jan. 1977 (JARE-17)	60	51	144	87
Feb. 1977–Jan. 1978 (JARE-18)	72	65	53	47
Feb. 1978–Jan. 1979 (JARE-19)	71	67	47	71
Feb. 1979–Jan. 1980 (JARE-20)	95	155	75	166
Feb. 1980–Jan. 1981 (JARE-21)	27	78	50	99

observations are classified as the sounder mode.

The Automatic Gain Control (AGC) voltage of the ISIS topside sounder receiver contains a spectral characteristics of noise with frequencies ranging from 100 kHz to 20 MHz (FRANKLIN and MACLEAN, 1969). Furthermore, ionograms provide the necessary information to relate the noise spectra to the distribution of the ionospheric plasma parameters determining the propagation mode or the generation condition in the noise source region.

This report is concerned with the spectral characteristics of the terrestrial radio noise in the low and medium frequency bands, above 100 kHz, appearing in the ISIS topside sounder data acquired at Syowa for the period from April 1976 to November 1977. In the next section several kinds of the noise bands are described and discussed stressing the comparison with the other observations thus far reported.

2. Observations of Terrestrial Kilometric Radiations

2.1. Noise events

The spectral characteristics of the noise band reported here were derived from ISIS-1 and -2 topside sounder data recorded at Syowa for the period from June 11, 1976 to November 30, 1977, and from April 14, 1976 to January 23, 1977, respectively. The total number of passes investigated amount to 88 for ISIS-1 and 138 for ISIS-2.

The ISIS-1 spacecraft is in an eccentric polar orbit with apogee and perigee heights of about 3510 km and 580 km, respectively, whereas ISIS-2 is in a polar orbit with an almost constant height of about 1400 km. Thus, ISIS-1 data is more suitable for examining the variety of the noise spectra in a broad range of altitudes over polar region. The LF/MF noise events observed during the above periods are summarized in Table 2 which shows occurrence time and location of the maximum noise intensity of the noise event observed along each ISIS pass. The maximum noise intensity is estimated from the AGC voltage level and the noise spectral structure. Remarks on the spectral features are also given in this table where "LFN" stands for radio noise having its upper frequency limit in LF band and its lower frequency limit near or below 100 kHz. "BN" means noise bands typically appearing between the local electron plasma frequency f_N and the upper hybrid resonance frequency f_T given by $(f_H^2+f_N^2)^{1/2}$, where f_H is the local electron gyrofrequency, or noise bands having a cutoff frequency closely associated with the local characteristic frequencies. "I" indicates noise whose intensity exceeds the saturation level of -60 dBm (JAMES, 1980). Among the events

Table 2. ISIS terrestrial kilometric radiation observations.

Date	UT (HM)	GMLT (HM)	HGT (km)	Inv. Lat (deg)	*Kp*	Remarks
ISIS-1, Syowa (Apr. 1976–Nov. 1977)						
1976						
Aug. 24	0553	0114	3400	79	4−	BN, NI
Sep. 6	1445	1103	2900	78	2−	BN+SN, I
Sep. 9	0233	1735	3080	85	3−	BN, NI
Sep. 22	0454	0949	2740	79	4−	LFN+BN, NI
Sep. 27	0904	0713	2040	76	3+	LFN+BN, NI
Sep. 30	0315	1019	2410	78	2	LFN+BN, NI
Oct. 6	0244	2219	1270	70	1+	BN→LFN, NI
Dec. 12	1750	1417	1270	72	4	LFN+BN, I
Dec. 13	1105	1536	1840	74	1+	LFN+BN, I
Dec. 14	1035	1501	1790	78	1−	LFN+BN, I
1977						
Mar. 7	2024	2021	3230	74	1−	BN+SN, I, TX-OFF
June 28	2032	0431	3080	64	3−	BN+SN, I
July 2	2044	0411	3100	69	3	BN+SN, I
July 3	2224	0207	3140	65	2−	BN+SN, I
July 20	0948	1412	2950	80	5−	BN+SN, I
Sep. 23	0238	0839	2350	82	3−	LFN, I, TX-OFF
ISIS-2, Syowa (Apr. 1976–Jan. 1977)						
1976						
Nov. 3	1736	1439	1450	73	1+	LFN+BN→BN, NI
Nov. 3	2124	1744	1450	69	3	LFN+BN→BN, NI
Dec. 1	1423	1215	1430	74	2+	LFN+BN→BN, NI
Dec. 3	1154	1324	1420	76	0+	LFN+BN→BN, NI
Dec. 4	1233	1353	1420	73	4	BN→LFN+BN→BN, NI
Dec. 5	1309	1302	1420	74	2	LFN+BN→BN, NI
Dec. 7	1230	1201	1420	75	2+	LFN+BN→BN, I, diffuse
Dec. 12	1342	1057	1420	74	4−	LFN+BN→BN, NI

LFN: Low Freq. Noise; BN: Banded Noise; SN: Sporadic Noise; NI: Not Intense; I: Intense

listed, all those indicated by "BN+SN" have been identified as auroral kilometric radiations (AKR) recently examined by several authors from various viewpoints using ISIS-1 sounder data and soft particle data (BENSON and CALVERT, 1979; BENSON *et al.*, 1980; CALVERT, 1981a; JAMES, 1980). Table 2 shows clearly the dependence of the spectral characteristics on altitude. Typical examples of noise characteristics are given below and are discussed in association with the other observations already reported.

2.2. *LF/MF noise at higher altitudes equal or greater than 1.4 R_E*

At altitudes above 2900 km, almost all noise bands observed are composed of intense terrestrial kilometric radiation labeled auroral kilometric radiation. The AKR is closely associated with discrete auroral arcs and is believed to originate on the field lines at radial distances ranging from 1.5 to 2.5 R_E in the nighttime magnetosphere (For a review, see GURNETT, 1978). Out of six AKR events, four events were observed in the nightside auroral zone and have similar characteristics with respect

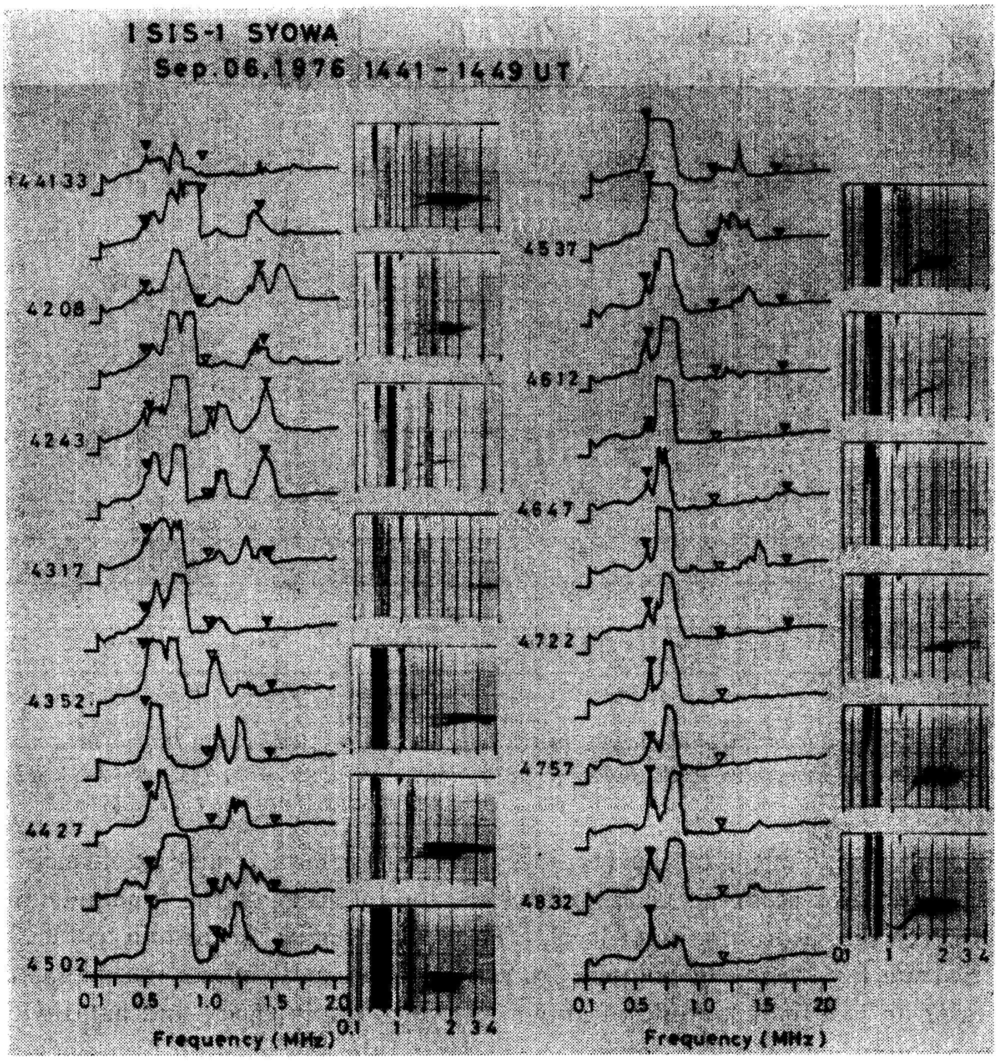

Fig. 1. A series of ISIS-1 Automatic Gain Control (AGC) data and corresponding ionograms showing AKR signals. These data were recorded at Syowa on September 6, 1976, between 1441–1449 UT. The fundamental and harmonics of gyrofrequency, f_H are indicated by three triangles.

to spectral structure related to the local plasma parameters, ranges of altitudes and invariant latitudes where these were observed, as previously reported. The latitudinal extent in which the other two events were observed indicates a close association with the magnetosheath particle precipitations in the dayside cusp region. As an example, Fig. 1 shows a series of 26 consecutive AGC sweeps of the ISIS-1 sounder receiver and the corresponding ionograms, recorded on September 6, 1976. As pointed out previously, the cusp-related AKR also exhibits a complex spectral structure (ALEXANDER and KAISER, 1977) with the lower cutoff frequency close to the local electron gyrofrequency, f_H. In this event the upper cutoff frequency of the widest band noise, 880 kHz, which appeared at 1445:02 UT is considerably higher than that reported by CALVERT (1981a). The fundamental noise bands are usually accompanied by some sporadically appearing harmonic noise bands. The relationship between these noise spectra and the harmonic frequency of the local f_H suggests that they may be

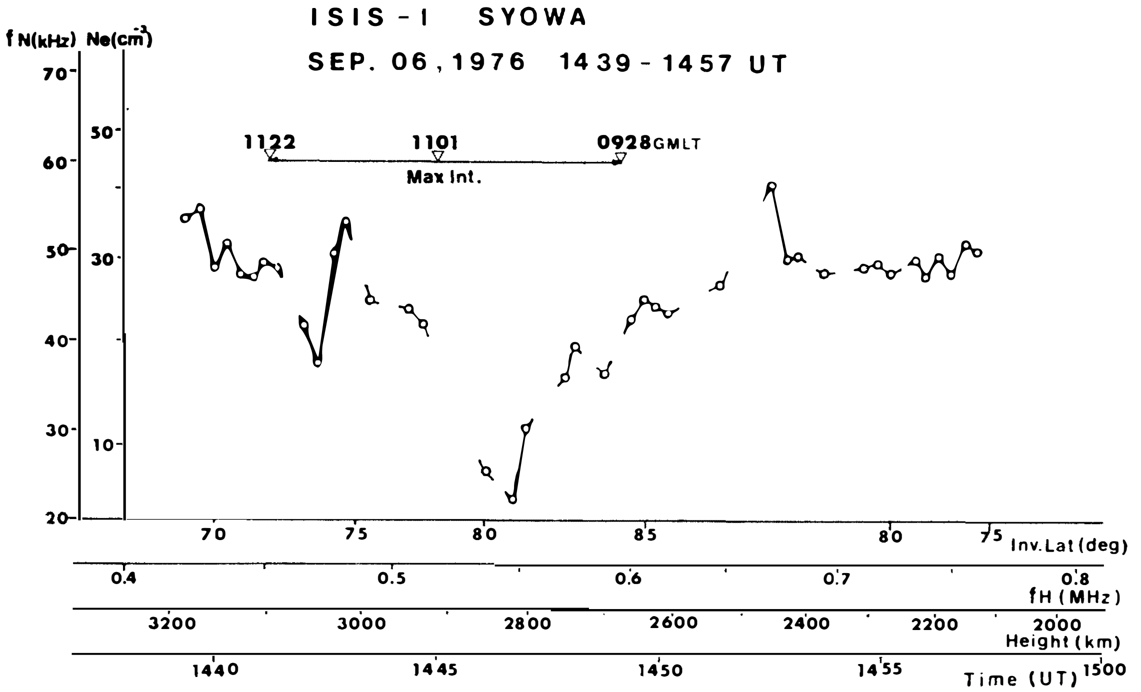

Fig. 2. The variation of local electron density along the pass as deduced by Hagg's beat method. The cusp-associated AKR signals given in Fig. 1 were observed at 1122–0928 GMLT.

due to a nonlinear effect of the receiver. This suggestion is also confirmed by the fact that this noise seems to occur only when the intensity of the fundamental noise band exceeds the saturating input level. The source region, according to the spectral analysis using ray tracing technique (CALVERT, 1981a), exists along the magnetic lines of force at an invariant latitude of about 78°, since the intensity and band width become maximum, and the gap between local f_H and the lower cutoff frequency reaches a minimum. As seen in the ionograms in Fig. 1, the local f_N is usually below the lower end of the sounder frequency sweep (100 kHz) and therefore cannot be directly scaled. In case of $f_T \simeq f_H$, that is, $f_N \ll f_H$ the beat patterns often appear resulting from intermodulation between f_T and f_H resonance spikes and give the relationship: $f_N \simeq (2f_i f_H)^{1/2}$ where f_i denotes a reciprocal of the dot period scaled on ionograms (HAGG, 1967). The variation of local f_N on this pass deduced by this technique is given in Fig. 2 along with the interval of AKR observation. Since the actual value of f_N may be statistically estimated to be about 10 percent higher than the one determined by the beat method (WHITTEKER, 1978), AKR signals appear to be observed over broad low electron density depletion interval with N_e less than 30 cm^{-3} except for a density enhancement around 1443 UT. In particular, there exits a pronounced trough with a minimum density of about 10 cm^{-3} centered around 81°INV. The most intense AKR appears to occur at the low latitude side of this density trough. The structure and the center latitude of this trough suggest an existence of an electron density cavity associated with AKR source in the dayside magnetosphere similar to that recently found by Hawkeye wave observation at geocentric distance from 1.8 R_E to 3.0 R_E in the nightside magnetosphere (CALVERT, 1981b). The ratio of f_N to f_H

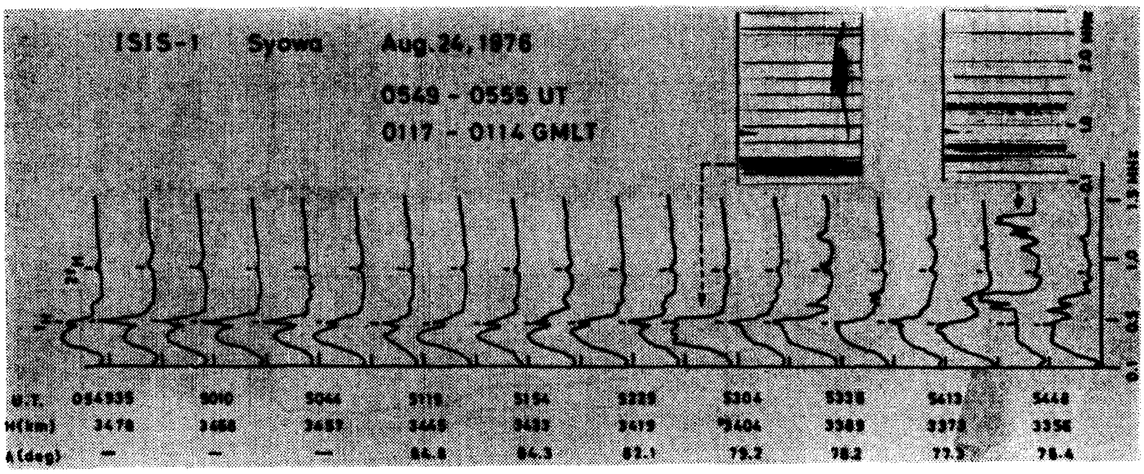

Fig. 3. A series of ISIS-1 AGC data and corresponding ionograms showing an example of the right-hand polarized Z mode emissions observed at altitudes near apogee. During this event the local f_N appears to be well below 100 kHz, from the beat method.

during this AKR event ranges from 0.1 to 0.05, indicating consistency with the values predicted and measured at or near the source region (ANDERSON *et al.*, 1981; CALVERT, 1981b; GRABBE, 1981).

At high altitudes near apogee, also observed were less intense noise bands at frequencies above local f_N. An example of such emissions are given in Fig. 3 which shows a sequence of AGC data and corresponding ionograms. This type of emission was weak and has a rather steady spectral structure over a wide latitudinal extent. Since at these altitudes local f_N is usually much less than 100 kHz, f_N cannot be determined on the ionograms. The application of the beat method to the ionogram at 0551 : 37 UT leads to $f_N \simeq 50$ kHz. The upper cutoff frequency of this noise band seems to be near local f_H which is approximately equal to local f_T and the lower frequency cutoff is not well-defined, indicating that this noise is quite different from the continuum radiation whose spectrum extends over a broad range of frequencies with a sharp lower frequency cutoff at the local f_N (GURNETT and GREEN, 1978). Rather, it should be interpreted as higher frequency components of the right-hand polarized Z mode wave which can exist between f_N and f_T, as will be described in the following section. This type of noise at high altitudes is too infrequent to draw more definite conclusions on mode indentification and various characteristics closely related to the source locations and the generation mechanism.

2.3. *LF/MF noise at altitudes less than about 1.4 R_E*

Below about 2900 km, the observed typical noise consists of the whistler mode noise of which upper frequency components can be detected by the sounder receiver, and the noise band appearing between the local f_N and f_T.

2.3.1. Whistler mode noise

As indicated in Table 2, the whistler mode noise events were observed at all altitudes below about 2900 km. This noise is rather common at low altitudes such as that of ISIS-2, although the noise level is not usually high enough to saturate the receiver. Three events of most intense noise were observed on three successive days

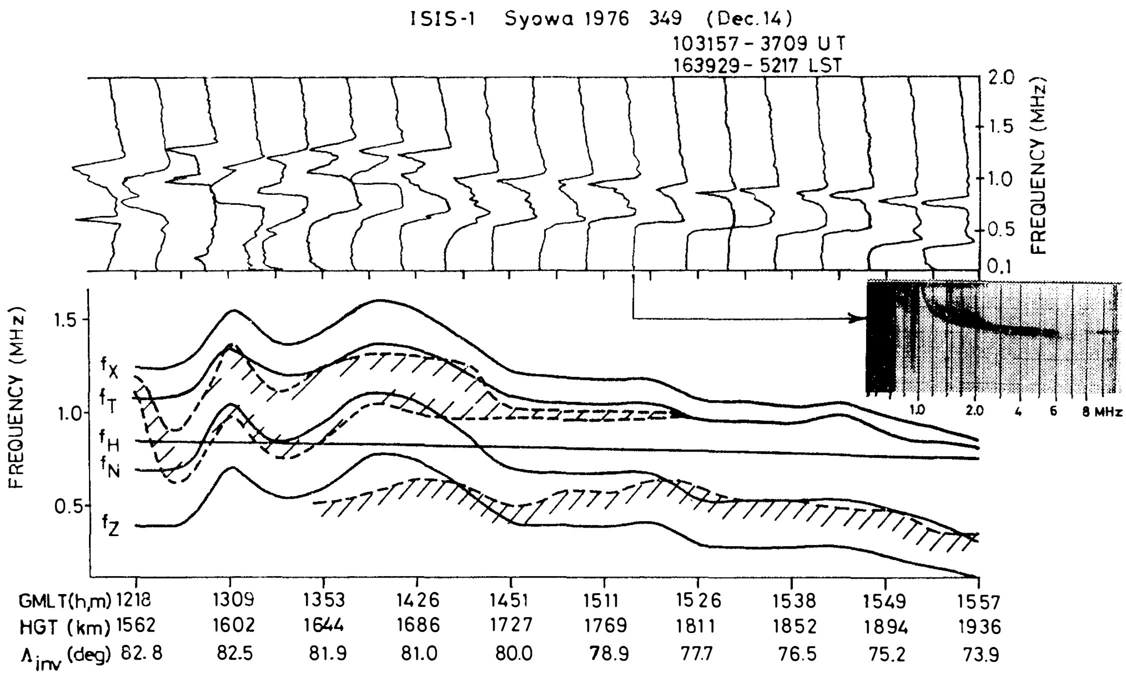

Fig. 4. A series of ISIS-1 AGC sweeps and the relationship between the frequency range of noise exceeding a certain threshold level and local characteristic frequencies f_N, f_H, f_T, f_X and f_Z scaled on ionograms. Two kinds of noise can be seen in these spectra.

from December 12 to 14, 1976. A typical example of one of these events is given in Fig. 4, showing a series of ISIS-1 AGC sweeps and the relationship between the frequency range of noise exceeding a certain threshold level and local characteristic frequencies; f_N, f_H, f_T, f_X and f_Z scaled on the ionograms, where f_X and f_Z are the X and Z mode cutoff frequencies at the satellite, given by $(f_N^2+f_H^2/4)^{1/2}+f_H/2$ and $(f_N^2+f_H^2/4)^{1/2}-f_H/2$, respectively. Also shown in the figure is an example of this noise appearing on an ionogram. In this event the noise has a remarkably sharp high frequency cutoff with frequencies around 500 kHz and extends down to frequencies less than 100 kHz. The most intense noise appears to be observed in the latitude interval of 80°–75° and maximum intensity occurred at about 78°INV, as estimated from the spectra. Since the upper cutoff frequency is affected neither by local f_Z nor f_N until it approaches f_N, this noise can be identified to be high frequency components of auroral hiss. During this event no auroral hiss in VLF band was observed at Syowa, located more than about 1900 km away from the subsatellite points. This implies that auroral hiss observable in the topside ionosphere is detectable over a limited area on the ground.

This event of Fig. 4 and the other two events recorded from December 12 to 14, 1976 occurred in the dayside topside ionosphere. Since the latitudinal extent in which the strongest noise intensity occurred agrees approximately with dayside cusp, these events may be attributed to the precipitating soft electrons with energy from 50 eV to 1 keV, often detected in the dayside cusp ionosphere (JAMES, 1973). However, the soft particle data from ISIS satellites unfortunately are not available for these events.

In Fig. 4, furthermore, a significant enhancement in local electron density can be discerned at latitudes near 81°INV. This cusp-related electron density enhancement is the most remarkable feature during very quiet condition ($Kp=1-$) and it is attributed to the upward expansion due to heating beneath the cusp (CHACKO and MENDILLO, 1977; WHITTEKER, 1976). It is interesting that in this case the local electron density enhancement occurred on the high latitude side of the cusp region in which the intense noises were observed. The invariant latitudinal width of the intense-noise region is about six degrees. The Kp dependence of the locations at which the most intense noise were recorded appears to be in good agreement with that of cusp locations statistically derived from the analysis of electron density distributions (TITHERIDGE, 1976). Furthermore, the occurrence region of the high intensity whistler mode noise events listed exists along almost the whole day and evening portion of the auroral oval.

Also in Fig. 6 is shown a typical example of this noise recorded on ISIS-2 data. The whistler mode noise was observed down to about 72°INV and has no well-defined high frequency cutoff. This event occurred likewise along the midday-afternoon sector of the auroral oval. This occurrence exhibits a pattern similar to that of northern high latitude region obtained by Alouette-2 (BARRINGTON *et al.*, 1971) and Ariel 3 (HUGHES *et al.*, 1971) observations.

The other example of the whistler mode noise is shown in Fig. 5, which was recorded in the early morning-midnight sector of the ionosphere (07–22 GMLT) when the sounder transmitter was not operating. This noise band has a sharp upper frequency cutoff near 400 kHz, well below the local f_H when the noise intensity is high enough to saturate the receiver. Although the local f_N cannot be scaled because of no f_N resonance spike, it can be reasonably supposed to be around the upper cutoff

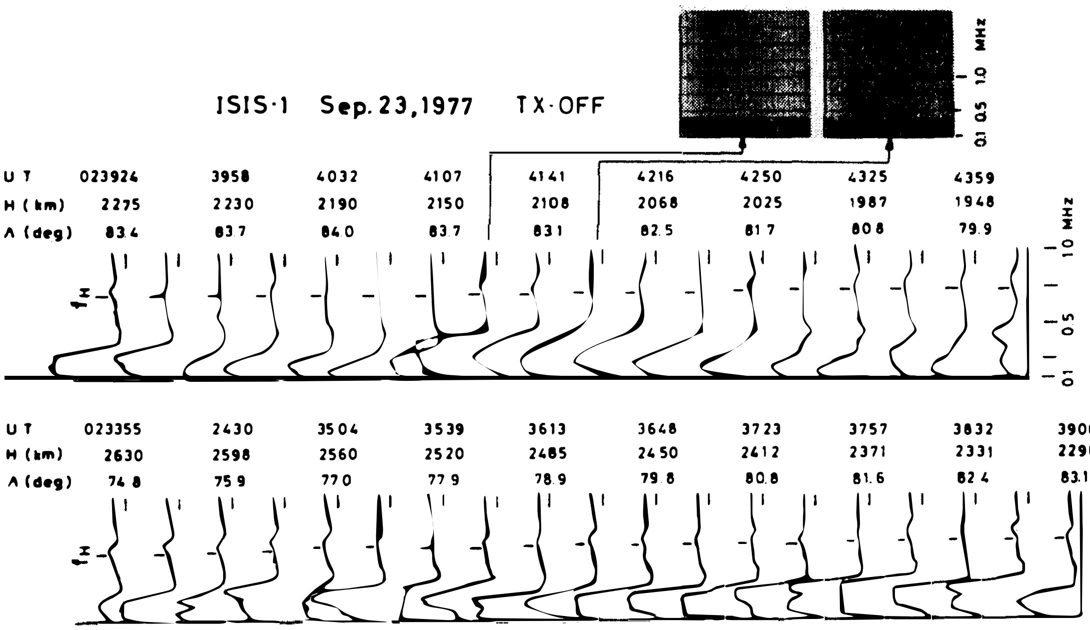

Fig. 5. A series of ISIS-1 AGC sweeps and two frames of ionograms showing intense whistler mode noise band recorded in the early morning-midnight sector of the ionosphere when the sounder transmitter was off. The local f_N is thought to be around the upper cutoff frequency of the noise band.

frequency considering the altitude, local time and *Kp* index. Insofar as the spectral structures are concerned, this noise is very similar to that frequently observed in the dayside (JAMES, 1973) and in the evening-midnight sector of the ionosphere (KISABETH and ROSTOKER, 1979). It should be noted, however, that the satellite trajectory during this event lies in the low intensity region of the LF band noise, as expressed in terms of the invariant latitude and local mean time (BARRINGTON *et al.*, 1971). This suggests that the noise source may be different from the field aligned current flow related to the discrete auroral arc as proposed by KISABETH and ROSTOKER (1979).

2.3.2. Banded noise with $f_N < f < f_T$

This type of noise has been reported by many authors on the basis of the satellite and rocket observations in the past two decades (*e.g.* HARTZ, 1969; MULDREW, 1970; MOSIER *et al.*, 1973, HANASZ *et al.*, 1976 and more recently MORIOKA *et al.*, 1981) and also can be seen in ISIS data in a broad range of latitudes over the southern polar region. Early results of ISIS-1 observation showed that this noise band is regularly observed in the high latitude ionosphere and the intensity is remarkably high, compared with that in the other regions (MULDREW, 1970). Typical examples of AGC traces of the noise bands observed by ISIS-1 and ISIS-2 on the sounder transmitter operating are shown in Figs. 4 and 6, respectively, along with a few ionograms. Almost all of the intense whistler mode noise events are always detected simultaneously with this type of noise as indicated in Table 2. The noise band, however, is not necessarily accompanied by the whistler mode noise and is observed in the broad latitudinal range below about 82°INV. When the transmitter is off, AGC traces exhibit relatively

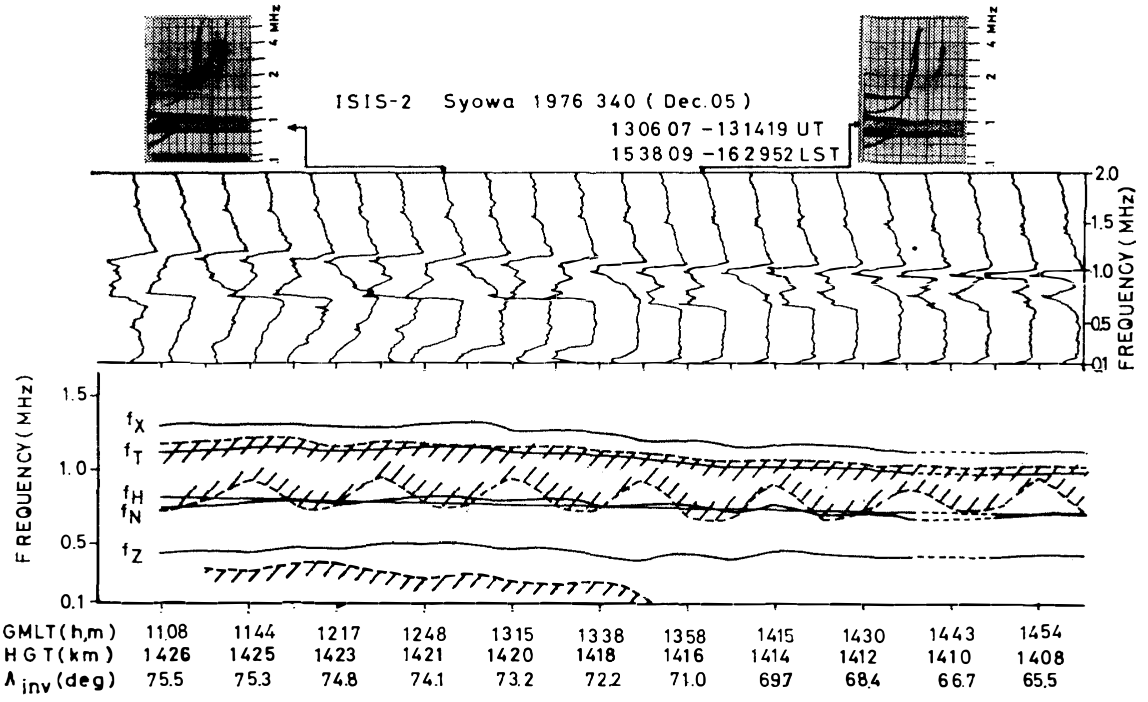

Fig. 6. A series of ISIS-2 AGC sweeps and the relationship between the noise band and the local characteristic frequencies. The periodic structure can be seen at the lower cutoff frequency of the noise band with $f_N < f < f_T$.

smooth curves with no sharp enhancement around local f_N and f_T. On the other hand, when the transmitter is on, signals with long duration excited by the sounder pulses often enhance the AGC voltage due to nonsynchronization of the integration start time with the sounder pulse timing, resulting in complication of the noise spectral structure between f_N and f_T, as is seen in the example traces. This makes it difficult to locate the peak intensity region necessary to relate the noise band to the other phenomena.

The early examination of Alouette-2 AGC recordings suggested the existence of two types of noise, *e.g.*, the noise bands with maximum amplitudes at around the local f_N and at around local f_T. These two types of noise show different dependence on the antenna orientation relative to the geomagnetic field. The noise with maximum intensity around f_N is affected by antenna orientation more strongly than other types of noise (HARTZ, 1969). This tendency can be seen in AGC traces in Fig. 6, where the lower frequency portions of the noise band have a periodic structure with a period of about 67 s. The discrepancy between this period and the half spin period ($\sim$10 s) seems to arise from the difference in the integration timing for AGC voltage and the spin phase.

The noise band shown in Fig. 4 has a noticeable tendency for the noise intensity in the region where f_N is greater than f_H to be considerably higher than that in the region of $f_N < f_H$. This feature is consistent with the power flux calculation of the electrostatic upper hybrid mode noise allowed for plausible auroral electron beam models (MAGGS, 1978) and suggests that the auroral electron beam of keV energies is one of the possible sources of this observed noise band at least in the auroral zone.

As pointed out by several authors, the antenna impedance strongly affected by the local plasma parameters must modify the amplitude and polarization characteristics of these noises, especially, at frequencies below local f_T. Furthermore, the AGC recordings include these components for both the electrostatic and the electromagnetic noise. Thus, the quantitative treatment of noise with such a frequency band needs at least information on magnetic components of the noise as well as the antenna impedance.

3. Summary

Preliminary analysis of the ISIS topside sounder data obtained at Syowa, Antarctica, for the period from April 1976 to November 1977 shows a variety of noise spectra on the sounder AGC data and ionograms. The noise events were observed on 16 out of 88 ISIS-1 passes and 8 out of 138 ISIS-2 passes. At altitudes above about 2900 km almost all noise events appeared to be auroral kilometric radiations whose characteristics have been examined recently by several authors using ISIS-1 data acquired over the arctic region. Out of six AKR events observed, two events are closely associated with magnetosheath particle precipitations in the dayside cusp. These cusp-related AKR show similar spectral structure and characteristics to those of AKR more frequently observed in the nightside.

At lower altitudes below about 2900 km, two kinds of noise were recorded; the whistler mode noise of which upper frequency component can be detected by the sounder receiver and the noise band appearing between f_N and f_T. Whereas the ISIS-1 observes various types of noise, almost all of noise observed by ISIS-2 are of these two types. Among these, the most intense noise event observed in the dayside was examined in conjunction with the local characteristic frequencies. The whistler mode noise of this event is found to have a spectrum with a sharp upper frequency cutoff and is identified as high frequency components of auroral hiss. For this event, the significant enhancement in local electron density associated with the cusp precipitation occurred on the high latitude side of the region where the most intense whistler mode noise was observed. In contrast to this, the noise band between f_N and f_T tends to be more intense in the density enhancement region. This feature can be explained qualitatively by the power flux calculations of electrostatic noise generated by auroral electron beams (Maggs, 1978).

Acknowledgments

The authors wish to express their thanks to Dr. J. H. Whitteker and Mr. J. D. R. Boulding, Communications Research Centre, Canada, NASA, USA and ISIS Working Group for their support to the ISIS topside sounder observation at Syowa, Antarctica. The authors are also grateful to the members of the 17th and 18th wintering parties of the Japanese Antarctic Research Expedition at Syowa for their collaboration in ISIS data acquisition.

References

Alexander, J. K. and Kaiser, M. L. (1977): Terrestrial kilometric radiation 2. Emission from the magnetospheric cusp and dayside magnetosheath. J. Geophys. Res., **82** (A1), 98–104.

Anderson, R. R., Calvert, W. and Gurnett, D. A. (1981): ISEE observations of auroral kilometric radiation in the source region; Abstract, AGU Spring Meeting. EOS, **62**, 359.

Barrington, R. E., Hartz, T. R. and Harvey, R. W. (1971): Diurnal distribution of ELF, VLF and LF noise at high latitudes as observed by Alouette 2. J. Geophys. Res., **76**, 5278–5291.

Benson, R. F. and Calvert, W. (1979): ISIS 1 observations at the source of auroral kilometric radiation. Geophys. Res. Let., **6**, 479–482.

Benson, R. F., Calvert, W. and Klumpar, D. M. (1980): Simultaneous wave and particle observations in the auroral kilometric radiation source region. Geophys. Res. Lett., **7**, 959–962.

Calvert, W. (1981a): The signature of auroral kilometric radiation on ISIS ionograms. J. Geophys. Res., **86**, 76–82.

Calvert, W. (1981b): The auroral plasma cavity. Geophys. Res. Lett., **8**, 919–921.

Chacko, C. C. and Mendillo, M. (1977): Electron density enhancements in the *F* region beneath the magnetospheric cusp. J. Geophy. Res., **82**, 4757–4764.

Franklin, C. A. and Maclean, M. A. (1969): The design of swept-frequency topside sounder. Proc. IEEE, **57**, 897–929.

Grabbe, C. L. (1981): Comment on "Direction of arrival measurements of auroral kilometric radiation and associated ELF data from Isis 1" by H. G. James. J. Geophys. Res., **86**(A3), 1645.

Gurnett, D. A. (1978): Electromagnetic plasma wave emissions from the auroral field lines. J. Geomagn. Geoelectr., **30**, 257–272.

Gurnett, D. A. and Green, J. L. (1978): On the polarization and origin of auroral kilometric radiation. J. Geophys. Res., **83**(A2), 689–693.

Hagg, E. L. (1967): Electron densities of 8–100 electrons cm^{-3} deduced from Alouette II high latitude ionograms. Can. J. Phys., **45**, 27–36.

HANASZ, J., SCHREIBER, R., AKSENOV, V. I., KOMRAKOV, G. P., WELNOWSKI, H. and WIKIERSKI, B. (1976): Naturally excited Bernstein mode at frequencies above the second harmonic of the electron gyrofrequency in the ionosphere. COSPAR Space Res., **17**, 493–497.

HARTZ, T. R. (1969): Radio noise levels within and above the ionosphere. Proc. IEEE, **57**, 1042–1050.

HUGHES, A. R. W., KAISER, T. R. and BULLOUGH, K. (1971): The frequency of occurrence of VLF radio emissions at high latitudes. COSPAR Space Res., **11**, 1323–1330.

JAMES, H. G. (1973): Whistler-mode hiss at low and medium frequencies in the dayside-cusp ionosphere. J. Geophys. Res., **78**, 4578–4599.

JAMES, H. G. (1980): Direction-of-arrival measurements of auroral kilometric radiation and associated ELF data from ISIS-1. J. Geophys. Res., **85**, 3367–3375.

KISABETH, J. L. and ROSTOKER, G. (1979): Relationship of noise in the frequency range $100<f<500$ kHz to auroral arcs and field-aligned current and implications regarding acceleration of auroral electron. J. Geophys. Res., **84**(A3), 853–868.

MAGGS, J. E. (1978): Electrostatic noise generated by the auroral electron beam. J. Geophys. Res., **83**, 3173–3188.

MATUURA, N., OGATA, T. and NISHIZAKI, R. (1977): Nankyokuiki ni okeru ISIS toppusaido saundingu (ISIS topside sounding above antarctic region). Proc. IMS Symp. held at Inst. Space Aero. Sci., 122–127.

MORIOKA, A., OYA, H. and MIYATAKE, S. (1981): Terrestrial kilometric radiation observed by satellite JIKIKEN (EXOS-B). J. Geomagn. Geoelectr., **33**, 37–62.

MOSIER, S. R., KAISER, M. L. and BROWN, L. W. (1973): Observations of noise bands associated with the upper hybrid resonance by the Imp 6 radio astronomy experiment. J. Geophys. Res., **78**, 1673–1679.

MULDREW, D. B. (1970): Preliminary results of Isis 1 concerning electron density variations, ionospheric resonances and Cerenkov radiation. COSPAR Space Res., **10**, 786–794.

TITHERIDGE, J. E. (1976): Ionospheric heating beneath the magnetospheric cleft. J. Geophys. Res., **81**, 3221–3226.

WHITTEKER, J. H. (1976): The magnetospheric cleft-Ionosphere effects. J. Geophys. Res., **81**, 1279–1288.

WHITTEKER, J. H. (1978): A comparison of the beat method of determining low electron densities from topside ionograms with the plasma-frequency resonance method. Radio Sci., **13**, 1047–1051.

(Received November 30, 1981; Revised manuscript received January 27, 1982)